

# Weak-Driven Learning: How Weak Agents make Strong Agents Stronger

Zehao Chen <sup>\*1,2</sup> Gongxun Li <sup>\*1,2</sup> Tianxiang Ai <sup>\*2</sup> Yifei Li <sup>1,2</sup> Zixuan Huang <sup>1</sup> Wang Zhou <sup>2</sup> Tao Huang <sup>2</sup>  
 Fuzhen Zhuang <sup>1</sup> Xianglong Liu <sup>1</sup> Jianxin Li <sup>1</sup> Deqing Wang <sup>1,†</sup> Yikun Ban <sup>1,†</sup>

## Abstract

As post-training optimization becomes central to improving large language models, we observe a persistent saturation bottleneck: once models grow highly confident, further training yields diminishing returns. While existing methods continue to reinforce target predictions, we find that informative supervision signals remain latent in models' own historical weak states. Motivated by this observation, we propose WMSS (Weak Agents Can Make Strong Agents Stronger), a post-training paradigm that leverages weak checkpoints to guide continued optimization. By identifying recoverable learning gaps via entropy dynamics and reinforcing them through compensatory learning, WMSS enables strong agents to improve beyond conventional post-training saturation. Experiments on mathematical reasoning and code generation datasets show that agents trained with our approach achieve effective performance improvements, while incurring zero additional inference cost. Code is available at <https://github.com/chenzehao82/Weak-Driven-Learning.git>.

## 1. Introduction

The dominant post-training paradigms, including Supervised Fine-Tuning (SFT) (Ouyang et al., 2022; Touvron et al., 2023; Zou et al., 2025; Chen et al., 2025), Knowledge Distillation (KD) (Hinton et al., 2015; Gou et al., 2021; Agarwal et al., 2023), and Curriculum Learning (Bengio et al., 2009; Xu et al., 2023), share a common principle: learning from stronger supervision signals. These approaches rely on a mimicking objective, training models to approximate high-quality labels or the outputs of a stronger teacher, under the assumption that closer alignment leads to improved performance.

<sup>\*</sup>Equal contribution <sup>†</sup>Corresponding Author <sup>1</sup>Beihang University <sup>2</sup>China Telecom eSurfing Cloud. If you have any questions, feel free to contact Yikun Ban <yikunb@buaa.edu.cn>, or Zehao Chen <gyy.chenzehao@chinatelecom.cn> or zehaochenacid@buaa.edu.cn>.

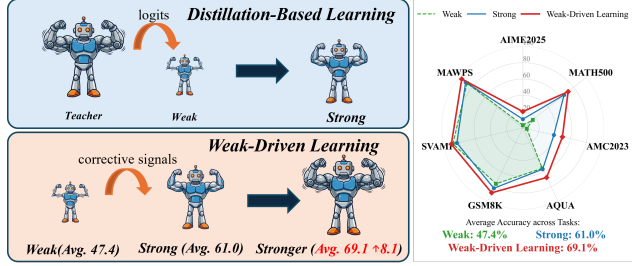


Figure 1. **Paradigm Comparison:** Distillation-Based Learning vs. Weak-Driven Learning.

While highly effective during early training, such paradigms are increasingly observed to suffer from performance saturation as optimization proceeds (Chen et al., 2024; Dong et al., 2024a). Specifically, the logit margin—defined as the gap between the target logit and the average non-target logits—grows rapidly in early epochs but stabilizes thereafter. Once this margin saturates, the decision boundary becomes effectively fixed, and gradients induced by standard supervised objectives diminish, limiting further improvement. Existing remedies, such as continued SFT or self-revision and reflection-based fine-tuning, have shown limited effectiveness in addressing this saturation bottleneck (Gudibande et al., 2023; Zhou et al., 2024; Huang et al., 2024; Stechly et al., 2024). Despite architectural or procedural differences, these methods still rely on reinforcing correct targets and therefore struggle to provide informative learning signals once supervised gradients vanish.

In this work, we approach this challenge from a fundamentally different perspective by introducing a new post-training paradigm, termed *Weak-Driven Learning*. Our approach is inspired by a common human learning phenomenon: in complex collaborative problem-solving, a strong individual working alongside a weaker teammate is often forced to further refine their reasoning in order to complete the task successfully. Crucially, this improvement does not arise from repeatedly applying the correct solution, but from observing, analyzing, and correcting the weaker teammate's mistakes. Such mistakes expose plausible yet incorrect reasoning paths that must be explicitly ruled out, thereby sharpening the distinction between correct and incorrect decisions.

Guided by this insight, we challenge the conventional as-

sumption that learning with weaker models necessarily degrades performance. Instead, we show that weak agents can provide informative error signals that continue to drive improvement even when standard supervision saturates. We formalize this principle as *Weak-Driven Learning*, capturing the idea that **Weak Agents can Make Strong Agents Stronger**. Unlike knowledge distillation, which depends on access to a stronger teacher that is often expensive or unavailable, weak-driven learning leverages weak reference models that are easy to obtain, such as historical checkpoints of the model itself.

As illustrated in Figure 1, weak-driven learning fundamentally inverts the conventional learning flow. Instead of transferring knowledge from a stronger teacher to a weaker student, a weak agent injects structured uncertainty and exposes failure modes that compel an already strong agent to further refine its decision boundary. By explicitly identifying and distancing the strong model from these failure modes, learning can continue beyond the saturation point of standard supervision. Rather than discarding early-stage checkpoints as inferior intermediates, our approach actively reuses them as a source of corrective supervision, enabling sustained model evolution without introducing additional inference cost.

To distinguish this paradigm clearly from existing post-training strategies, we now provide a formal definition of Weak-Driven Learning.

#### Definition: Weak-Driven Learning

*Weak-Driven Learning* refers to a class of post-training paradigms in which the improvement of a strong model is driven by systematic discrepancies between its predictions and those of a weaker reference model (e.g., a historical checkpoint), rather than by imitation of a stronger teacher.

Formally, given a strong agent  $\mathcal{M}_{\text{strong}}$ , a weak agent  $\mathcal{M}_{\text{weak}}$ , and a task dataset  $\mathcal{D}$ , weak-driven learning constructs training signals by jointly leveraging the outputs of  $\mathcal{M}_{\text{strong}}$  and  $\mathcal{M}_{\text{weak}}$  on  $\mathcal{D}$ . These joint signals are then used to further optimize the strong agent. As a result, the strong agent  $\mathcal{M}_{\text{strong}}$  is updated into a stronger agent  $\mathcal{M}_{\text{strong}}^+$  with improved task performance.

Our contributions are summarized as follows:

**Learning paradigm.** We introduce *Weak-Driven Learning*, a new post-training paradigm that highlights the overlooked role of weak agents—such as historical model checkpoints—as driving signals that can further improve strong agents.

**Training framework.** We propose WMSS, a practical post-training framework that operationalizes weak-driven

learning through joint optimization of weak and strong models via logit mixing. This mechanism compels the strong model to refine its decision boundary and sustain meaningful gradients in saturated regimes, without additional inference overhead.

**Theoretical analysis.** We provide a gradient-level analysis of the joint training mechanism, theoretically demonstrating how incorporating weak-model logits reshapes the optimization landscape, prevents gradient vanishing on non-target tokens, and maintains effective learning pressure beyond standard supervision.

**Empirical performance.** We empirically demonstrate that WMSS consistently improves performance on challenging benchmarks, including mathematical reasoning and code generation, compared to standard SFT baselines. These gains arise purely from improved optimization dynamics during training and incur no additional inference cost.

## 2. Related Work

**Post-training Paradigms: From SFT to Knowledge Distillation.** Supervised Fine-Tuning (SFT) has established itself as the cornerstone of aligning Large Language Models (LLMs) (Ouyang et al., 2022; Touvron et al., 2023; Yang et al., 2026; Huang et al., 2026; He et al., 2025). To further enhance efficiency, Knowledge Distillation (KD) is frequently integrated into post-training. Traditional approaches, including standard KD (Hinton et al., 2015) and Self-Distillation methods (Zhang et al., 2019; Xu et al., 2023), typically operate on a premise of *mimicry*: the model is optimized to approximate a “superior” distribution, derived either from a larger teacher or its own smoothed predictions. Recent LLM-specific variants like GKD (Agarwal et al., 2023) and MiniLLM (Gu et al., 2023) refine this by addressing distribution mismatch, yet they retain the core “Strong-to-Weak” or “Self-Smoothing” logic. While effective for knowledge transfer, these mimicry-based objectives share a critical limitation with SFT where the diminishing supervisory gradients near convergence lead to optimization saturation and logit rigidification. In contrast, WMSS abandons the mimicry objective. We utilize historical weak checkpoints not as targets to approximate, but as sources of structured uncertainty to reactivate gradients, thereby breaking the optimization saturation barrier where SFT and standard KD stagnate.

**Weak-to-Strong Generalization & Supervision.** The potential for weak supervisors to elicit superior capabilities has attracted significant interest. Burns et al. (Burns et al., 2023) formalized the phenomenon of “weak-to-strong generalization,” demonstrating that strong models can generalize beyond the imperfect labels provided by weaker supervisors. This paradigm has been further extended to iterative

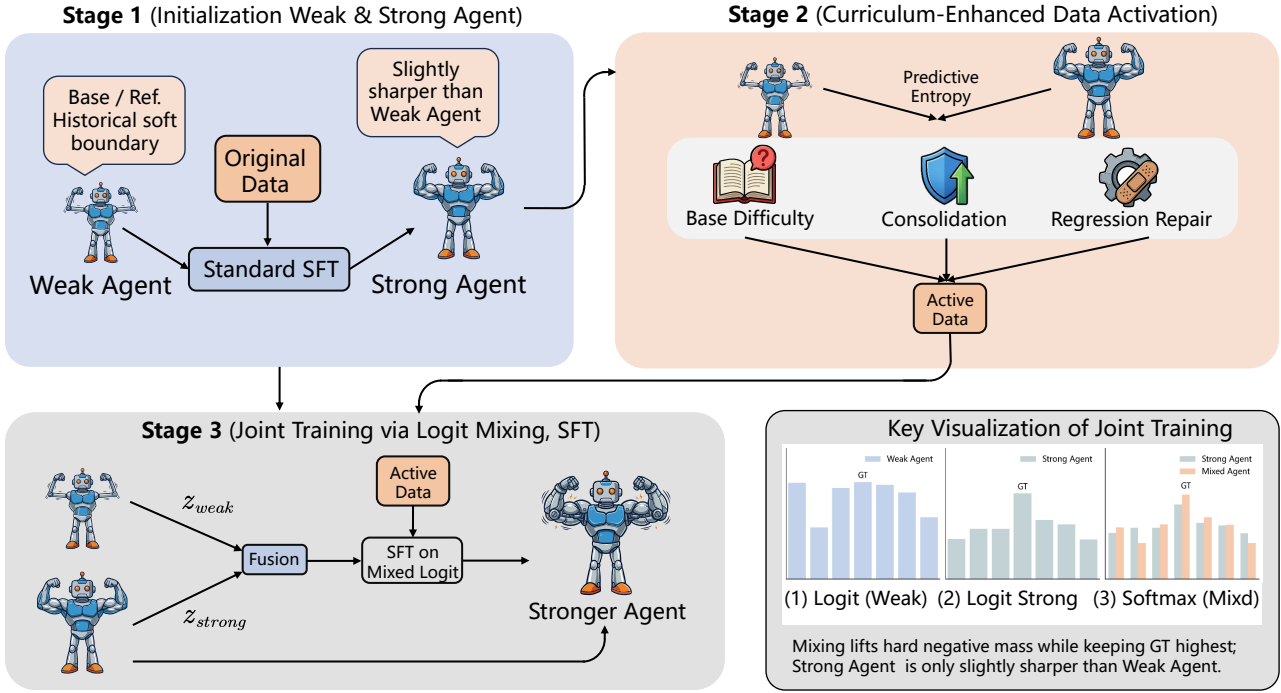


Figure 2. Weak-Driven Learning. Overview of WMSS. The framework has three phases: (1) initialization, (2) activate SFT data via curriculum learning, and (3) jointly train weak and strong models to obtain a stronger model; The right panel visualizes the joint-training principle through logit mixing and gradient amplification.

self-improvement (Gulcehre et al., 2023). Unlike these methods which focus on elicitation in the absence of ground truth, WMSS addresses *optimization saturation* in fully supervised settings. We utilize historical weak logits not as targets to follow, but as corrective signals to sustain gradient flow.

### 3. Preliminaries

We consider an autoregressive language model  $\mathcal{M}_\theta$  that maps a context sequence  $x$  to a next-token distribution over a vocabulary  $\mathcal{V}$ . At decoding step  $t$ , the model outputs logits  $z_t \in \mathbb{R}^{|\mathcal{V}|}$ , which induce a probability distribution

$$P_\theta(\cdot | x) = \text{Softmax}(z_t). \quad (1)$$

**Supervised fine-tuning.** In standard supervised fine-tuning (SFT), we minimize the negative log-likelihood over a dataset  $\mathcal{D}$ :

$$\mathcal{L}_{\text{SFT}}(\theta) = -\mathbb{E}_{(x,y) \sim \mathcal{D}} [\log P_\theta(y | x)] \quad (2)$$

where  $y$  denotes the ground-truth next token under context  $x$  (we omit the time index when clear).

**Predictive entropy.** To quantify uncertainty and diagnose optimization stagnation, we monitor the predictive entropy

of the next-token distribution:

$$H(P_\theta(\cdot | x)) = - \sum_{v \in \mathcal{V}} P_\theta(v | x) \log P_\theta(v | x). \quad (3)$$

Let  $\ell(x, y; \theta) = -\log P_\theta(y | x)$  be the per-token cross-entropy loss. Its gradient w.r.t. the logit of any token  $k \in \mathcal{V}$  is

$$\frac{\partial \ell}{\partial z_t[k]} = P_\theta(k | x) - \mathbb{I}[k = y]. \quad (4)$$

In particular, for any negative token  $k \neq y$ , we have

$$\left| \frac{\partial \ell}{\partial z_t[k]} \right| = P_\theta(k | x) \quad (5)$$

i.e., the gradient magnitude on a negative class is proportional to its assigned probability. Weak-driven learning explicitly leverages this property: by reintroducing probability mass to plausible but suppressed alternatives through logit mixing, it amplifies informative gradients on unresolved decision regions, thereby sustaining effective optimization beyond the supervised saturation regime.

### 4. How Can Weak Make Strong Stronger

In this section, we describe how a weak agent can be leveraged to further strengthen a strong agent.

**Weak and strong agent initialization.** In WMSS, the weak agent  $\mathcal{M}_{\text{weak}}$  (a.k.a.  $\mathcal{M}_{\text{ref}}$ ) is initialized from the base checkpoint and co-trained with the strong agent during joint training. We begin with **Phase 1 (Initialization)**: starting from a base model  $\mathcal{M}_0$ , we perform standard SFT to obtain  $\mathcal{M}_1$ , and set

$$\mathcal{M}_{\text{weak}} \leftarrow \mathcal{M}_0, \quad \mathcal{M}_{\text{strong}} \leftarrow \mathcal{M}_1. \quad (6)$$

The weak agent provides a corrective signals via its logits

$$z_{\text{weak}}(x) \in \mathbb{R}^{|\mathcal{V}|} \quad (7)$$

which preserve a softer decision boundary and highlight plausible distractors (non-target tokens), stabilizing continued optimization.

#### 4.1. Curriculum-Enhanced Data Activation

At this stage, training data for the strong agent  $\mathcal{M}_{\text{strong}}$  is constructed via a curriculum-enhanced data activation process guided by the weak reference  $\mathcal{M}_{\text{weak}}$ . Rather than uniformly sampling from a fixed corpus, we use the weak-strong model pair to diagnose uncertainty dynamics on individual samples and selectively activate data that is most informative for continued learning.

**Entropy dynamics.** For each sample  $x_i$ , define predictive entropy under model  $\mathcal{M}$  as

$$H(\mathcal{M}; x_i) = H(P_{\mathcal{M}}(\cdot | x_i)). \quad (8)$$

We measure how uncertainty changes from the weak reference to the current strong agent by

$$\Delta H_i = H(\mathcal{M}_{\text{strong}}; x_i) - H(\mathcal{M}_{\text{weak}}; x_i). \quad (9)$$

Here,  $H(\mathcal{M}_{\text{weak}}; x_i)$  captures *historical difficulty*, while  $\Delta H_i$  indicates whether the strong agent has become more certain (learned) or more uncertain (regressed) than the weak reference.

**Curriculum construction.** We sample training examples using a mixture of three entropy-based signals:

$$p_i \propto \alpha H(\mathcal{M}_{\text{weak}}; x_i) + \beta [-\Delta H_i]_+ + \gamma [\Delta H_i]_+ \quad (10)$$

where  $[u]_+ := \max(u, 0)$  and normalization is over  $i$ . The three terms have an intuitive role:

- **Base difficulty** ( $\alpha$ ). Up-weights samples that the weak reference found uncertain, ensuring inherently hard concepts remain emphasized.
- **Consolidation** ( $\beta$ ). If  $\Delta H_i < 0$ , the strong agent is more certain than the weak reference; large decreases can indicate fast but brittle learning, so we revisit these samples to stabilize retention.

- **Regression repair** ( $\gamma$ ). If  $\Delta H_i > 0$ , the strong agent is less certain than the weak reference. Since the weak model handled the sample better, this is strong evidence the sample is learnable (not irreducible noise) and indicates regression/catastrophic forgetting; we up-weight such samples to recover the lost boundary.

The resulting curriculum-enhanced data activation yields the training set for the subsequent stage, in which explicit weak guidance is incorporated during training.

#### 4.2. Weak-Driven Learning: Joint Training of Weak and Strong

The core operation of WMSS is Joint Training: given a weak agent  $\mathcal{M}_{\text{weak}}$  and a strong agent  $\mathcal{M}_{\text{strong}}$ , we convert the weak agent’s reference signals into additional optimization pressure, driving the strong agent toward an even stronger checkpoint  $\mathcal{M}_{\text{strong}}^+$  through gradient amplification. This realizes the principle *Weak + Strong  $\rightarrow$  stronger Strong*.

**Joint training via logit mixing.** For a training pair  $(x, y)$ , let  $z_{\text{strong}}(x), z_{\text{weak}}(x) \in \mathbb{R}^{|\mathcal{V}|}$  denote the next-token logits produced by  $\mathcal{M}_{\text{strong}}$  and  $\mathcal{M}_{\text{weak}}$ , respectively. We construct a joint probability map by linearly mixing the logits:

$$z_{\text{mix}}(x) = \lambda z_{\text{strong}}(x) + (1 - \lambda) z_{\text{weak}}(x), \quad (11)$$

where  $\lambda \in [0, 1]$ . We then optimize the strong agent using the mixed-logit distribution  $P_{\text{mix}}(\cdot | x) := \text{Softmax}(z_{\text{mix}}(x))$ :

$$\mathcal{L}_{\text{mix}} = -\mathbb{E}_{(x, y) \sim \mathcal{D}} [\log P_{\text{mix}}(y | x)] \quad (12)$$

Gradients propagate through  $z_{\text{mix}}$  via standard backpropagation. Intuitively, the weak agent assigns non-negligible probability mass to plausible but incorrect tokens that the strong agent may have already suppressed. By mixing logits, these hard negatives are reintroduced under  $P_{\text{mix}}$ , preventing their associated gradients from vanishing. This mechanism reactivates informative learning signals in saturated regions of the decision space, enabling continued refinement of the strong agent’s decision boundary.

#### 4.3. Training Pipeline

Algorithm 1 summarizes WMSS.

**Phase 1 (Initialization)** trains  $\mathcal{M}_0$  with SFT to obtain  $\mathcal{M}_{\text{strong}}$  and initializes  $\mathcal{M}_{\text{weak}} \leftarrow \mathcal{M}_0, \mathcal{M}_{\text{strong}} \leftarrow \mathcal{M}_1$ . **Phase 2 (Curriculum)** constructs an active training distribution by computing entropy dynamics between  $\mathcal{M}_{\text{weak}}$  and the current  $\mathcal{M}_{\text{strong}}$ , yielding a curriculum-weighted dataset  $\mathcal{D}_{\text{active}}$  via Eq. (10).

**Phase 3 (Weak-driven Training)** then performs joint training on  $\mathcal{D}_{\text{active}}$  by mixing logits as in Eq. (11) and optimizing

**Algorithm 1** Weak Agents make Strong Agents Stronger

**Require:** Dataset  $\mathcal{D}$ , Base Model  $\mathcal{M}_0$   
**Require:** Iterations  $K$ , Hyperparams  $\lambda$

```

1: Phase 1: Initialization
2:  $\mathcal{M}_1 \leftarrow \text{Train}(\mathcal{M}_0, \mathcal{D}, \mathcal{L}_{\text{SFT}})$ 
3: Phase 2: Iterative Training Loop
4: for  $t = 1$  to  $K$  do
5:   // Step A: Curriculum-Enhanced Data Activation
6:    $\Delta \mathbf{H} \leftarrow \mathbf{H}(\mathcal{M}_t) - \mathbf{H}(\mathcal{M}_{t-1})$ 
7:   Calculate  $\mathbf{p}$  via Eq. 10 using  $\Delta \mathbf{H}$  and  $\mathbf{H}(\mathcal{M}_{t-1})$ 
8:    $\mathcal{D}_{\text{active}} \leftarrow \text{WeightedSample}(\mathcal{D}, \mathbf{p})$ 
9:   // Step B: Weak-Driven Learning
10:  Initialize  $\mathcal{M}_\theta \leftarrow \mathcal{M}_t$ 
11:  for batch  $(x, y) \in \mathcal{D}_{\text{active}}$  do
12:     $z_{\text{weak}} \leftarrow \text{Forward}(\mathcal{M}_{t-1}, x)$ 
13:     $z_{\text{strong}} \leftarrow \text{Forward}(\mathcal{M}_\theta, x)$ 
14:     $z_{\text{mix}} \leftarrow \lambda z_{\text{strong}} + (1 - \lambda) z_{\text{weak}}$ 
15:    Update  $\mathcal{M}_\theta$  via  $\nabla \text{CE}(z_{\text{mix}}, y)$ 
16:  end for
17:   $\mathcal{M}_{t+1} \leftarrow \mathcal{M}_\theta$ 
18: end for
19: return  $\mathcal{M}_{K+1}$ 

```

the mixed-logit cross-entropy loss in Eq. (12). This allows  $\mathcal{M}_{\text{strong}}$  to suppress weak-revealed distractors and continue strengthening beyond saturation, producing  $\mathcal{M}_{\text{strong}}^+$ .

## 5. Why Can Weak Make Strong Stronger

In this section, we formalize the key advantage of weak-driven learning: **joint logit mixing with a weak agent amplifies informative gradients in saturated regions**, enabling continued optimization of strong agent beyond standard supervised fine-tuning. We show that, by reintroducing probability mass to plausible but suppressed alternatives, joint training prevents gradient vanishing on non-target tokens and sustains effective learning pressure even after the strong model’s decision boundary has stabilized.

### 5.1. Why Joint Training Amplifies Gradients in Saturated Regions

Consider a weak agent  $\mathcal{M}_{\text{weak}}$  (initialized from a historical checkpoint and co-trained during joint training) and a strong agent  $\mathcal{M}_{\text{strong}}$  (current trainable agent) that, for a context  $x$ , produce logits  $z_{\text{weak}}(x), z_{\text{strong}}(x) \in \mathbb{R}^{|\mathcal{V}|}$  over the vocabulary  $\mathcal{V}$ , and the mixed logits

$$z_{\text{mix}}(x) = (1 - \lambda)z_{\text{weak}}(x) + \lambda z_{\text{strong}}(x), \quad \lambda \in [0, 1]. \quad (13)$$

Operationally,  $z_{\text{mix}}(x)$  is the fused logit map used for joint training, injecting the weak agent’s uncertainty while preserving the strong agent’s target direction. Let  $y$  denote the target index,  $e_y$  the one-hot vector, and define  $P_{\text{mix}}(\cdot | x) = \text{Softmax}(z_{\text{mix}}(x))$  and  $P_{\text{strong}}(\cdot | x) =$

$\text{Softmax}(z_{\text{strong}}(x))$ . More generally, for any logit map  $z(x)$ , let  $P_z(\cdot | x) = \text{Softmax}(z(x))$ . The cross-entropy gradient on fused logits is

$$g_{\text{mix}} = \nabla_{z_{\text{mix}}(x)} \mathcal{L} = P_{\text{mix}}(\cdot | x) - e_y, \quad (14)$$

For any negative token  $k \neq y$ , the gradient component is  $g_{\text{mix}}[k] = P_{\text{mix}}(k | x)$ , so increasing negative probability mass directly increases the gradient magnitude on that token. Standard SFT on the strong agent gives  $g_{\text{sf}} = P_{\text{strong}}(\cdot | x) - e_y$  and can saturate when  $P_{\text{strong}}(k | x)$  is already small.

**Margins and hard negatives.** Define the target margin for any negative token  $k \neq y$  as

$$m_k(z(x)) = z(x)[y] - z(x)[k]. \quad (15)$$

The margin measures target-vs-distractor separation: smaller margins mean higher confusion. We define the hard-negative set

$$\mathcal{H} = \{k \neq y : m_k(z_{\text{weak}}(x)) < m_k(z_{\text{strong}}(x))\}. \quad (16)$$

These are tokens where the weak agent is less separated than the strong agent, i.e., the weak agent highlights unresolved boundaries. The mixed margin is a convex combination:

$$m_k(z_{\text{mix}}(x)) = (1 - \lambda)m_k(z_{\text{weak}}(x)) + \lambda m_k(z_{\text{strong}}(x)). \quad (17)$$

Thus mixing shrinks margins toward the weak agent on  $\mathcal{H}$ , raising the relative probability of hard negatives.

**Theorem 5.1** (Total negative-mass increase under uniform margin shrinkage). *If  $m_k(z_{\text{weak}}(x)) \leq m_k(z_{\text{strong}}(x))$  for all  $k \neq y$ , then*

$$\begin{aligned} P_{\text{mix}}(y | x) &\leq P_{\text{strong}}(y | x), \\ \sum_{k \neq y} P_{\text{mix}}(k | x) &\geq \sum_{k \neq y} P_{\text{strong}}(k | x). \end{aligned} \quad (18)$$

The theorem shows that, when the weak agent is uniformly more uncertain than the strong agent, joint logit mixing necessarily shifts probability mass from the target to negative tokens. As a consequence, gradient magnitude on negative classes is amplified, preventing vanishing gradients in saturated regions. This mechanism explains why weak-driven learning enables continued refinement of the strong agent’s decision boundary even after standard supervised fine-tuning has converged. A complete proof is provided in Appendix B.

**Corollary 5.2** (Per-token amplification on hard negatives). *For any  $k \in \mathcal{H}$ , the mixed negative gradient satisfies*

$$\begin{aligned} P_{\text{mix}}(k | x) &\geq P_{\text{strong}}(k | x) \quad \text{whenever} \\ \frac{P_{\text{mix}}(y | x)}{P_{\text{strong}}(y | x)} &\geq \exp(-(1 - \lambda)\Delta m_k), \end{aligned} \quad (19)$$

where  $\Delta m_k = m_k(z_{\text{strong}}(x)) - m_k(z_{\text{weak}}(x)) > 0$ .

This corollary provides a token-level characterization of gradient amplification: for hard negatives, joint logit mixing increases their assigned probability—and thus their gradient magnitude, under mild and explicit conditions on the relative target probabilities.

**Proposition 5.3** (Logit updates on negative and target tokens). *Under joint training, for agent  $i \in \{\text{weak, strong}\}$  with scale  $s_{\text{weak}} = 1 - \lambda$ ,  $s_{\text{strong}} = \lambda$ ,*

$$\begin{aligned}\Delta z_{i,k} &\approx -\eta s_i P_{\text{mix}}(k \mid x) \quad (k \neq y), \\ \Delta z_{i,y} &\approx \eta s_i (1 - P_{\text{mix}}(y \mid x)).\end{aligned}\quad (20)$$

Thus any increase in  $P_{\text{mix}}(k \mid x)$  directly amplifies suppression of hard negatives, while a decrease in  $P_{\text{mix}}(y \mid x)$  strengthens the upward push on the target logit.

The proposition shows that any increase in the mixed probability  $P_{\text{mix}}(k \mid x)$  directly amplifies the suppressive update on non-target tokens, while a corresponding decrease in  $P_{\text{mix}}(y \mid x)$  strengthens the upward update on the target logit. These dynamics are consistent with the empirical reduction of the non-target logit mean observed in our logit statistics.

#### Summary (Why Weak-Driven Learning Works):

These theoretical results formalize the key advantage of weak-driven learning over standard SFT. By redistributing probability mass toward hard negatives in saturated regions, joint logit mixing with a weak agent increases gradient magnitudes for the strong agent that would otherwise vanish under SFT. While the dominant effect arises from amplified suppression of non-target tokens, the concurrent reduction in target probability further strengthens the positive update on the correct class. Together, these effects alleviate optimization saturation and enable the strong agent to continue refining its decision boundary beyond the convergence point of conventional supervised fine-tuning.

Mechanistic interpretation (three stages) of weak-driven learning:

**Stage I: saturated-region amplification.** Early in joint training, the weak agent is more confused on many non-target tokens, so mixing increases total negative mass (Appendix B, Eq. (39));  $g_{\text{mix}}$  is biased toward hard negatives, and the strong agent dominates the effective update (Appendix C, Eq. (70)).

**Stage II: gradient shielding.** As the strong agent becomes confident, the Softmax Hessian collapses (Appendix C, Eq. (76)) and the cross-Hessian between agents vanishes (Eq. (75)). The weak agent then receives little curvature information, so its influence on training diminishes even though it still provides the fused logits.

**Stage III: null-space drift.** Because Softmax is invariant to global logit shifts (Eq. (78)), the loss is flat along the mean

direction. When gradients are small, stochastic updates can drift in this null space, producing the observed mean-logit drift without changing centered sharpness (Appendix C).

## 6. Experiments

We conduct extensive experiments to evaluate the effectiveness and efficiency of our proposed method. First, we evaluate WMSS’s performance on two representative tasks, math reasoning and code generation.

**Arithmetic & Code Generation Datasets.** To comprehensively evaluate WMSS, we utilize a broad suite of reasoning tasks: (i) Arithmetic reasoning: AIME2025, MATH500, AMC23, AQuA (Ling et al., 2017), GSM8K (Cobbe et al., 2021), MAWPS (Koncel-Kedziorski et al., 2016), and SVAMP (Patel et al., 2021). (ii) Code Generation: HumanEval (Chen et al., 2021), MBPP (Austin et al., 2021).

**Implementation Details.** For WMSS, we employ models from both the Qwen family (Qwen3-4B-Base, Qwen3-8B-Base) (Yang et al., 2025) as the backbone. We utilize the AM-1.4M dataset (Zhao et al., 2025) for supervised fine-tuning. All experiments are conducted on eight NVIDIA H800 GPUs. Our training pipeline is implemented based on the TRL library, utilizing the Qwen3 architecture from the transformers library. We configure the global learning rate to  $1 \times 10^{-5}$  and set the maximum sequence length to 8192 to accommodate complex reasoning chains. Regarding the hyperparameters of WMSS, we use  $\alpha = 0.1$ ,  $\beta = 0.8$ , and  $\gamma = 0.1$ . Furthermore, for logit mixing, we set the mixing coefficient to  $\lambda = 0.5$  to balance the weak and strong logits in the joint-training loss.

**Baselines.** To evaluate the effectiveness of WMSS, we compare it against several competitive fine-tuning strategies:

- **Standard SFT:** The conventional supervised fine-tuning paradigm that optimizes the standard next-token prediction objective. It serves as a deterministic reference, devoid of any curriculum strategies or logit-space noise injection mechanisms.
- **UNDIAL**(Dong et al., 2024b): A method that subtracts a one-hot vector scaled by random Gaussian noise from the target token’s logits to suppress specific outputs..
- **NEFTune** (Jain et al., 2023): A robust noise-injection baseline that adds random noise to the embedding vectors during training. Following the original implementation, we set the noise scaling hyperparameter  $\alpha = 5$ .

To ensure a fair comparison, all other experimental configurations—including the learning rate, maximum sequence

**Table 1. Main Results on Qwen3-4B-Base and Qwen3-8B-Base.** We benchmark WMSS against standard SFT, UNDIAL and NEFTune across 7 math datasets and 2 code datasets. All models are fine-tuned for a total of 2 epochs, and all reported results are averaged over 3 runs. **Bold** indicates the best performance, and underline denotes the second best.

Methods	Math								Code		
	AIME2025	MATH500	AMC23	AQUA	GSM8K	MAWPS	SVAMP	Avg.	HumanEval	MBPP	Avg.
<i>Qwen3-4B-Base as base model.</i>											
SFT	12.2	66.1	<b>47.7</b>	<u>61.8</u>	83.9	91.3	85.5	64.1	68.5	<b>57.7</b>	63.1
UNDIAL	12.2	63.1	40.0	<u>55.1</u>	82.9	90.9	84.1	61.2	71.3	54.6	63.0
NEFTune	<u>16.7</u>	<b>68.2</b>	43.3	58.9	<b>86.7</b>	<u>93.8</u>	<u>87.7</u>	<u>65.0</u>	<u>74.2</u>	55.1	<b>64.7</b>
WMSS	<b>20.0</b>	<b>71.3</b>	<b>50.0</b>	<b>67.6</b>	<b>88.5</b>	<b>96.2</b>	<b>90.3</b>	<b>69.1</b>	<b>74.4</b>	<b>59.2</b>	<b>66.8</b>
<i>Qwen3-8B-Base as base model.</i>											
SFT	<u>15.6</u>	72.1	<b>45.0</b>	63.0	87.5	95.1	88.6	66.7	78.3	64.0	71.2
UNDIAL	10.0	71.5	48.3	66.9	89.9	96.4	91.2	67.7	79.7	61.0	70.4
NEFTune	<u>15.6</u>	<b>73.7</b>	40.0	<u>71.3</u>	<u>90.3</u>	<u>97.3</u>	<u>91.5</u>	<u>68.5</u>	<u>80.5</u>	<u>64.3</u>	<b>72.4</b>
WMSS	<b>20.0</b>	<b>75.4</b>	<b>52.5</b>	<b>77.3</b>	<b>92.5</b>	<b>97.8</b>	<b>94.0</b>	<b>72.9</b>	<b>83.9</b>	<b>71.3</b>	<b>77.6</b>
<i>Qwen2.5-3B as base model.</i>											
SFT	2.2	46.9	21.6	51.3	76.6	<u>91.6</u>	84.4	53.5	51.4	<b>42.7</b>	47.1
UNDIAL	<u>4.4</u>	50.7	18.3	<u>49.3</u>	77.4	91.3	83.2	53.5	50.8	42.5	46.7
NEFTune	2.2	<u>51.3</u>	<u>22.5</u>	47.1	<u>78.1</u>	90.3	<u>84.7</u>	<u>53.7</u>	<u>51.8</u>	41.5	46.7
WMSS	<b>5.5</b>	<b>52.0</b>	<b>22.5</b>	<b>53.8</b>	<b>80.9</b>	<b>92.6</b>	<b>86.0</b>	<b>56.2</b>	<b>53.7</b>	<b>43.3</b>	<b>48.5</b>

length, and optimizer settings—are kept strictly consistent with those used in WMSS.

## 6.1. Main Results

Table 1 shows that WMSS consistently breaks the optimization plateau of standard SFT across both model scales and task domains. On Qwen3-4B-Base, standard SFT reaches 64.1% accuracy on math reasoning, whereas WMSS improves performance to 69.1%, yielding a **+5.0%** absolute gain. A similar improvement is observed on code generation, where accuracy increases from 63.1% to 66.8%. These gains further scale with model capacity. On Qwen3-8B-Base, WMSS raises math accuracy from 66.7% to 72.9% (**+6.2%**), and improves code generation performance from 71.2% to 77.6%. Overall, the consistent improvements across both math and code tasks suggest that WMSS enhances general reasoning capabilities rather than being confined to a single domain.

**Adaptive Gains across Difficulty Regimes.** A deeper breakdown reveals that WMSS acts as an adaptive regularizer across both model scales. The improvements are most profound on *Hard* and competition-level tasks: on AIME2025, WMSS boosts the SFT(Qwen3-4B-Base) baseline from 12.2% to **20.0%** and lifts SFT(Qwen3-8B-Base) from 15.6% to **20.0%**. This capability is further reinforced on AMC23, where our method steadily improves the 4B model (47.7% → **50.0%**) and delivers a substantial leap on the 8B model (45.0% → **52.5%**), recovering from the dip observed in standard SFT. On *Medium* tasks like AQUA, WMSS effectively rectifies optimiza-

tion issues, with Qwen3-8B-Base exhibiting a massive gain (63.0% → **77.3%**) and Qwen3-4B-Base showing robust growth (61.8% → **67.6%**). Even on *Easy* benchmarks (e.g., MAWPS), both models push towards saturation (reaching 96.2% and 97.8% respectively) without suffering from catastrophic forgetting.

**WMSS vs. UNDIAL.** We compare WMSS against the UNDIAL baseline to evaluate the optimal strategy for logit adjustment. While UNDIAL focuses on **directly suppressing the target token** via stochastic penalties, Table 1 reveals that this approach degrades performance (Avg **-1.4%**). This suggests that naively penalizing the ground truth disrupts the primary training signal. In sharp contrast, WMSS achieves robust gains (surpassing the baseline by **7.9%** on Qwen3-4B-Base Math). This validates that distractors creates a more effective gradient signal than dampening the target itself, as it refines the decision boundary by widening the margin between the correct prediction and competing errors without sacrificing confidence in the ground truth.

**WMSS vs. NEFTune.** We benchmark WMSS against NEFTune to contrast *targeted correction* with *blind regularization*. NEFTune mitigates overfitting by injecting random noise into embeddings, which encourages the model to rely on pre-trained knowledge rather than memorization. However, it remains agnostic to the model’s specific error patterns. In contrast, WMSS leverages historical confusion to construct structurally informed corrective signals. This methodological divergence leads to consistent performance gains on held-out test sets. In particular, WMSS signif-

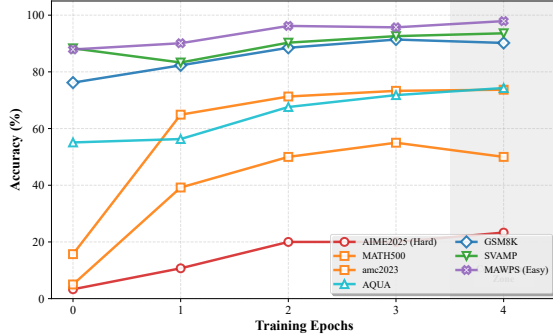


Figure 3. Convergence Analysis across Tasks. The training trajectory of WMSS (Qwen3-4B-Base) over 4 epochs.

icantly outperforms NEFTune on math reasoning benchmarks (69.1% vs. 65.0% on Qwen3-4B-Base; see Table 1), indicating that generic regularization alone is insufficient for harder reasoning tasks. These results suggest that overcoming the bottlenecks of mathematical reasoning requires structurally aligned guidance rather than purely stochastic perturbations.

## 6.2. Convergence Analysis across Tasks

Figure 3 visualizes training trajectories across seven datasets, revealing a two-stage pattern: rapid acquisition followed by asymptotic stabilization. While substantial gains occur within the first three epochs, marginal utility diminishes thereafter. Crucially, we observe **over-optimization** in the final stages; notably, **AMC2023** (brown line) exhibits sharp regression after Epoch 3, while **GSMSK** shows volatility. This identifies **Epoch 4** as the critical inflection point to maximize generalization before the onset of catastrophic forgetting.

## 6.3. Statistical Analysis: Why WMSS Works

As visualized in Figure 4, standard SFT optimization inevitably encounters a saturation bottleneck where the model loses the gradient drive to distinguish valid tokens from distractors: the target logits hit a ceiling (plateauing at 35.88), while the non-target logits cease to decline ( $z_{bg}$  sticking at 2.09). WMSS breaks this deadlock through a distinct “suppression-dominant” mechanism (i.e., the non-target logit mean drops more than the target logit rises) detailed in Table 2. Rather than relying on forcing the already high target logits higher (showing only a marginal +0.6% increase), our method aggressively suppresses background interference (the non-target logit mean ( $z_{bg}$ )), precipitating a dramatic 56.9% reduction in the Non-Target Logit Mean ( $z_{bg}$  :  $2.09 \rightarrow 0.90$ ). This suppression effectively “clears the signal path,” expanding the Target-to-Background Gap ( $\Delta_{gap}$ ) by +1.41 points; crucially, due to the exponential nature of the Softmax function ( $P \propto e^z$ ), this linear expansion is significantly amplified in probability space, resulting

Table 2. Logit Dynamics Analysis (Qwen3-4B-Base). Comparison of logit statistics at Epoch 3. Values in parentheses indicate the relative change of WMSS vs. SFT.

Metric	SFT	WMSS
Target Strength ( $z_{target}$ )	35.88	36.10 (+0.6%)
Distractors Mean ( $z_{bg}$ )	2.09	<b>0.90</b> (-56.9%)
Target-to-Background Gap ( $\Delta_{gap}$ )	33.79	<b>35.20</b> (+4.2%)
Logit Variance ( $\sigma$ )	2.93	3.45 (+17.7%)

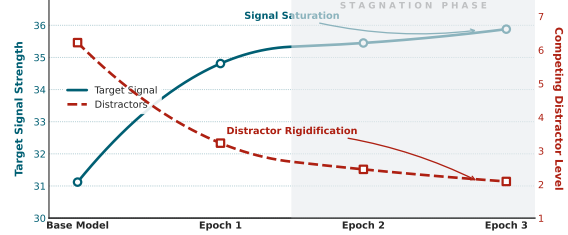


Figure 4. Limits of SFT Logit Growth on Qwen3-4B-Base. After an initial growth phase, both correct and incorrect token logits saturate, preventing standard SFT from further enlarging their margin.

in sharper decision boundaries and the robust performance gains observed in our experiments.

## 6.4. Ablation Study

Table 3 deconstructs the incremental contributions within the WMSS framework. The **CEDA** module first establishes a robust foundation by filtering high-value samples, improving the average accuracy by +2.2% (54.1%  $\rightarrow$  56.3%), though its impact on the challenging AIME task remains limited (12.2%  $\rightarrow$  13.3%). The addition of **JTWS** marks a critical turning point, utilizing corrective signals to bridge the reasoning gap and lifting the average accuracy to 58.2%. Finally, the full model achieves maximal robustness, peaking at **59.9%** on average and nearly doubling the baseline performance on AIME (**20.0%**). This progression confirms that while data curation provides a necessary baseline, the synergistic integration of weak-to-strong signals is essential for overcoming the optimization bottlenecks in complex mathematical reasoning.

## 7. Conclusion

In this work, we introduced WMSS, a training paradigm that fundamentally **inverts the traditional distillation logic**. Rather than relying on stronger teachers, we demonstrate that *weak* historical checkpoints harbor critical corrective signals required to break the optimization stagnation of standard SFT. By structurally leveraging these signals to amplify gradients from hard negatives, our method achieves remarkable scalability, notably **doubling performance on**

**Table 3. Ablation on Qwen3-4B-Base.** The **Baseline** denotes standard SFT. We incrementally add **CEDA** (Curriculum-Enhanced Data Activation.) and **JTWS** (Joint Training of Weak and Strong). WMSS represents the full model (Baseline + CEDA + JTWS).

Method	AIME	MATH500	GSM8K	Avg.
Baseline	12.2	66.1	83.9	54.1
+ CEDA	13.3	69.4	86.2	56.3
+ JTWS	16.7	70.2	87.6	58.2
WMSS	<b>20.0</b>	<b>71.3</b>	<b>88.5</b>	<b>59.9</b>

**AIME2025.** Beyond these benchmarks, our findings offer a proof-of-concept for **autonomous self-evolution**: effective alignment does not strictly demand external supervision or larger models. Instead, the “waste” of training—historical confusion and distractors—can be repurposed as the fuel for breaking performance ceilings. This opens a new, data-efficient frontier for post-training large language models, suggesting that the key to stronger agents may lie in understanding their weaker selves.

## Impact Statement

This paper presents a paradigm shift in post-training optimization by introducing **Weak-Driven Learning**, which challenges the conventional assumption that supervision must originate from a superior source. By demonstrating that strong models can transcend optimization plateaus using signals from weaker historical checkpoints, our work suggests a pathway toward more autonomous and scalable model evolution, particularly in the context of Weak-to-Strong Generalization. This approach provides an alternative to standard supervised fine-tuning and reduces reliance on expensive high-quality annotations or computationally heavy teacher models. This paper presents work whose goal is to advance the field of Machine Learning. While there are many potential societal consequences of our work, none are identified that must be specifically highlighted beyond those commonly associated with large language models.

## References

Agarwal, R., Vieillard, N., Stanczyk, P., Ramos, S., Geist, M., and Bachem, O. Gkd: Generalized knowledge distillation for auto-regressive sequence models. *CorR*, 2023.

Austin, J., Odena, A., Nye, M., Bosma, M., Michalewski, H., Dohan, D., Jiang, E., Cai, C., Terry, M., Le, Q., et al. Program synthesis with large language models. *arXiv preprint arXiv:2108.07732*, 2021.

Bengio, Y., Louradour, J., Collobert, R., and Weston, J. Curriculum learning. In *Proceedings of the 26th annual international conference on machine learning*, pp. 41–48, 2009.

Burns, C., Izmailov, P., Kirchner, J. H., Baker, B., Gao, L., Aschenbrenner, L., Chen, Y., Ecoffet, A., Joglekar, M., Leike, J., et al. Weak-to-strong generalization: Eliciting strong capabilities with weak supervision. *arXiv preprint arXiv:2312.09390*, 2023.

Chen, L., Li, S., Yan, J., Wang, H., Gunaratna, K., Yadav, V., Kumar, Z., Liu, Y., Parikh, D., and Xu, S. Alpagasus: Training a better alpaca with fewer data. In *The Twelfth International Conference on Learning Representations*, 2024.

Chen, M., Tworek, J., Jun, H., Yuan, Q., de Oliveira Pinto, H. P., Kaplan, J., Edwards, H., Burda, Y., Joseph, N., Brockman, G., Ray, A., Puri, R., Krueger, G., Petrov, M., Khlaaf, H., Sastry, G., Mishkin, P., Chan, B., Gray, S., Ryder, N., Pavlov, M., Power, A., Kaiser, L., Bavarian, M., Winter, C., Tillet, P., Such, F. P., Cummings, D., Plappert, M., Chantzis, F., Barnes, E., Herbert-Voss, A., Guss, W. H., Nichol, A., Paino, A., Tezak, N., Tang, J., Babuschkin, I., Balaji, S., Jain, S., Saunders, W., Hesse, C., Carr, A. N., Leike, J., Achiam, J., Misra, V., Morikawa, E., Radford, A., Knight, M., Brundage, M., Murati, M., Mayer, K., Welinder, P., McGrew, B., Amodei, D., McCandlish, S., Sutskever, I., and Zaremba, W. Evaluating large language models trained on code, 2021. URL <https://arxiv.org/abs/2107.03374>.

Chen, Z., Ai, T., Li, Y., Li, G., Wei, Y., Zhou, W., Li, G., Yu, B., Chen, Z., Sun, H., et al. Llmboost: Make large language models stronger with boosting. *arXiv preprint arXiv:2512.22309*, 2025.

Cobbe, K., Kosaraju, V., Bavarian, M., Chen, M., Jun, H., Kaiser, L., Plappert, M., Tworek, J., Hilton, J., Nakano, R., et al. Training verifiers to solve math word problems. *arXiv preprint arXiv:2110.14168*, 2021.

Dong, G., Yuan, H., Lu, K., Li, C., Xue, M., Liu, D., Wang, W., Yuan, Z., Zhou, C., and Zhou, J. How abilities in large language models are affected by supervised fine-tuning data composition. In *Proceedings of the 62nd Annual Meeting of the Association for Computational Linguistics (Volume 1: Long Papers)*, pp. 177–198, 2024a.

Dong, Y. R., Lin, H., Belkin, M., Huerta, R., and Vulić, I. Undial: Self-distillation with adjusted logits for robust unlearning in large language models, 2024b. URL <https://arxiv.org/abs/2402.10052>.

Gou, J., Yu, B., Maybank, S. J., and Tao, D. Knowledge distillation: A survey. *International Journal of Computer Vision*, 129(6):1789–1819, March 2021. ISSN 1573-1405. doi: 10.1007/s11263-021-01453-z. URL <http://dx.doi.org/10.1007/s11263-021-01453-z>.

Gu, Y., Dong, L., Wei, F., and Huang, M. Minillm: Knowledge distillation of large language models. *arXiv preprint arXiv:2306.08543*, 2023.

Gudibande, A., Wallace, E., Snell, C., Geng, X., Liu, H., Abbeel, P., Levine, S., and Song, D. The false promise of imitating proprietary llms, 2023. URL <https://arxiv.org/abs/2305.15717>.

Gulcehre, C., Paine, T. L., Srinivasan, S., Konyushkova, K., Weerts, L., Sharma, A., Siddhant, A., Ahern, A., Wang, M., Gu, C., Macherey, W., Doucet, A., Firat, O., and de Freitas, N. Reinforced self-training (rest) for language modeling, 2023. URL <https://arxiv.org/abs/2308.08998>.

He, X., Ban, Y., Zou, J., Wei, T., Cook, C., and He, J. Llm-forest: Ensemble learning of llms with graph-augmented prompts for data imputation. In *Findings of the Association for Computational Linguistics: ACL 2025*, pp. 6921–6936, 2025.

Hinton, G., Vinyals, O., and Dean, J. Distilling the knowledge in a neural network. *arXiv preprint arXiv:1503.02531*, 2015.

Huang, J., Chen, X., Mishra, S., Zheng, H. S., Yu, A. W., Song, X., and Zhou, D. Large language models cannot self-correct reasoning yet, 2024. URL <https://arxiv.org/abs/2310.01798>.

Huang, Z., Xia, X., Ren, Y., Zheng, J., Xiao, X., Xie, H., Huaiqiu, L., Liang, S., Dai, Z., Zhuang, F., Li, J., Ban, Y., and Wang, D. Real-time aligned reward model beyond semantics, 2026. URL <https://arxiv.org/abs/2601.22664>.

Jain, N., yeh Chiang, P., Wen, Y., Kirchenbauer, J., Chu, H.-M., Somepalli, G., Bartoldson, B. R., Kailkhura, B., Schwarzschild, A., Saha, A., Goldblum, M., Geiping, J., and Goldstein, T. Neftune: Noisy embeddings improve instruction finetuning, 2023. URL <https://arxiv.org/abs/2310.05914>.

Koncel-Kedziorski, R., Roy, S., Amini, A., Kushman, N., and Hajishirzi, H. Mawps: A math word problem repository. In *Proceedings of the 2016 conference of the north american chapter of the association for computational linguistics: human language technologies*, pp. 1152–1157, 2016.

Ling, W., Yogatama, D., Dyer, C., and Blunsom, P. Program induction by rationale generation: Learning to solve and explain algebraic word problems. *arXiv preprint arXiv:1705.04146*, 2017.

Ouyang, L., Wu, J., Jiang, X., Almeida, D., Wainwright, C., Mishkin, P., Zhang, C., Agarwal, S., Slama, K., Ray, A., et al. Training language models to follow instructions with human feedback. *Advances in neural information processing systems*, 35:27730–27744, 2022.

Patel, A., Bhattacharya, S., and Goyal, N. Are nlp models really able to solve simple math word problems? *arXiv preprint arXiv:2103.07191*, 2021.

Stechly, K., Valmeekam, K., and Kambhampati, S. On the self-verification limitations of large language models on reasoning and planning tasks, 2024. URL <https://arxiv.org/abs/2402.08115>.

Touvron, H. et al. Llama 2: Open foundation and fine-tuned chat models. *arXiv preprint arXiv:2307.09288*, 2023.

Xu, C., Sun, Q., Zheng, K., Geng, X., Zhao, P., Feng, J., Tao, C., and Jiang, D. Wizardlm: Empowering large language models to follow complex instructions. *arXiv preprint arXiv:2304.12244*, 2023.

Yang, A., Li, A., Yang, B., Zhang, B., Hui, B., Zheng, B., Yu, B., Gao, C., Huang, C., Lv, C., Zheng, C., Liu, D., Zhou, F., Huang, F., Hu, F., Ge, H., Wei, H., Lin, H., Tang, J., Yang, J., Tu, J., Zhang, J., Yang, J., Yang, J., Zhou, J., Zhou, J., Lin, J., Dang, K., Bao, K., Yang, K., Yu, L., Deng, L., Li, M., Xue, M., Li, M., Zhang, P., Wang, P., Zhu, Q., Men, R., Gao, R., Liu, S., Luo, S., Li, T., Tang, T., Yin, W., Ren, X., Wang, X., Zhang, X., Ren, X., Fan, Y., Su, Y., Zhang, Y., Zhang, Y., Wan, Y., Liu, Y., Wang, Z., Cui, Z., Zhang, Z., Zhou, Z., and Qiu, Z. Qwen3 technical report, 2025. URL <https://arxiv.org/abs/2505.09388>.

Yang, F., Chen, Z., Wang, X., Lu, X., Chai, J., Yin, G., Lin, W., Ma, S., Zhuang, F., Wang, D., Yang, Y., Li, J., and Ban, Y. Your group-relative advantage is biased, 2026. URL <https://arxiv.org/abs/2601.08521>.

Zhang, L., Song, J., Gao, A., Chen, J., Bao, C., and Ma, K. Be your own teacher: Improve the performance of convolutional neural networks via self distillation, 2019. URL <https://arxiv.org/abs/1905.08094>.

Zhao, H., Wang, H., Peng, Y., Zhao, S., Tian, X., Chen, S., Ji, Y., and Li, X. 1.4 million open-source distilled reasoning dataset to empower large language model training, 2025. URL <https://arxiv.org/abs/2503.19633>.

Zhou, C., Liu, P., Xu, P., Iyer, S., Sun, J., Mao, Y., Ma, X., Efrat, A., Yu, P., Yu, L., et al. Lima: Less is more for alignment. *Advances in Neural Information Processing Systems*, 36, 2024.

Zou, J., Ban, Y., Li, Z., Qi, Y., Qiu, R., Yang, L., and He, J. Transformer copilot: Learning from the mistake log in llm fine-tuning. *arXiv preprint arXiv:2505.16270*, 2025.

Table 4. Hyperparameter Sensitivity Analysis on Qwen3-4B-Base. We evaluate the impact of the mixing coefficients  $\alpha$  (base difficulty),  $\beta$  (consolidation), and  $\gamma$  (regression repair) on mathematical reasoning. **Bold** denotes the best performance.

Setup	Coefficients			Accuracy (%)	
	$\alpha$	$\beta$	$\gamma$	AIME 2025	MATH 500
Config A	0.2	0.7	0.1	10.0	68.2
<b>Ours (Selected)</b>	<b>0.1</b>	<b>0.8</b>	<b>0.1</b>	<b>16.7</b>	68.2
Config B	0.2	0.6	0.2	10.7	67.8
Config C	0.1	0.9	0.0	10.3	<b>70.2</b>
Config D	0.0	1.0	0.0	9.7	68.3
Config E	0.05	0.85	0.1	14.0	69.5

## A. Additional Experiments

### A.1. Sensitivity of Curriculum, Consolidation, and Repair Coefficients.

We further investigate the impact of the curriculum coefficient  $\alpha$ , the consolidation coefficient  $\beta$ , and the regression-repair coefficient  $\gamma$ . Table 4 presents the results on Qwen3-4B-Base. We observe a distinct trade-off between standard mathematical proficiency (MATH 500) and complex reasoning capability (AIME 2025).

Configuration C ( $\alpha = 0.1, \beta = 0.9, \gamma = 0$ ), which disables the regression-repair signal, achieves the highest accuracy on MATH 500 (**70.2%**). However, its performance on the more challenging AIME benchmark drops significantly to 10.3%. This suggests that while strong consolidation of the target distribution ( $\beta = 0.9$ ) helps with standard problems, it leads to optimization stagnation on harder tasks.

In contrast, our selected configuration ( $\alpha = 0.1, \beta = 0.8, \gamma = 0.1$ ) introduces a controlled regression-repair emphasis. Although this slightly reduces MATH performance (70.2%  $\rightarrow$  67.5%), it yields a decisive **+6.4%** gain on AIME (10.3%  $\rightarrow$  16.7%). This confirms that the additional gradient signal induced by  $\gamma$  is essential for breaking through reasoning bottlenecks, justifying our choice of parameters.

### A.2. Sensitivity Analysis on Mixing Coefficient $\lambda$

The mixing coefficient  $\lambda$  explicitly controls the relative weight between the weak and strong models in joint training, with fused logits  $z_{\text{mix}} = (1 - \lambda)z_1 + \lambda z_2$ . Smaller  $\lambda$  assigns more influence to the weaker model, while larger  $\lambda$  emphasizes the stronger model's direct fit to the targets.

We sweep  $\lambda$  over  $[0.1, 0.9]$  with a finer grid in  $[0.4, 0.6]$ . Table 5 shows a broad inverted U-shape: the best average performance occurs at  $\lambda = 0.42$  (Avg. 75.5%), and a strong plateau persists in  $\lambda \in [0.42, 0.48]$ . All benchmarks are evaluated with three-run averages; minor fluctuations on small sets (e.g., AIME25, 30 problems) are still expected, but the optimal region remains stable.

At the extremes, the behavior aligns with the mechanism. As  $\lambda \rightarrow 1$ ,  $z_{\text{mix}} \approx z_2$  and the joint training reduces to relying on the strong model, so the compensatory interaction weakens and accuracy drops (e.g., Avg. 67.6% at  $\lambda = 0.9$ ). As  $\lambda \rightarrow 0$ , the weak model dominates the fused logits, reducing effective target learning and risking underfitting; this is especially pronounced for weaker base models (e.g., at  $\lambda = 0.3$ , a weaker model attains only 13% accuracy on MATH500).

**Numerical consistency with the gradient-share crossover.** Following the theoretical analysis in Appendix C, we can estimate the effective sensitivity ratio using the centered-norm proxy:

$$\alpha \approx \left( \frac{\|\tilde{z}_2\|_2}{\|\tilde{z}_1\|_2} \right)^2. \quad (21)$$

From the logits evaluation report,  $\|\tilde{z}_2\|_2 \approx 1240.10$  and  $\|\tilde{z}_1\|_2 \approx 1034.50$ , giving  $\alpha \approx 1.44$ . Plugging into the crossover formula in Eq. (71),

$$\lambda_{\text{cross}} \approx \frac{1}{1 + \sqrt{\alpha}} \approx 0.455, \quad (22)$$

which lies close to the empirically strongest region ( $\lambda \in [0.42, 0.48]$ ). We stress that this is a *heuristic consistency check*:  $\alpha$  is phase-dependent and the linearization is local, so the theory predicts a broad optimum region rather than a sharp inversion point.

**Table 5. Sensitivity Analysis of Mixing Coefficient  $\lambda$ .** We report the accuracy (%) on Qwen3-4B-Base across varying  $\lambda$  values. The curve exhibits a broad inverted U-shape, with the strongest performance typically in the  $\lambda \in [0.42, 0.48]$  range (peak at  $\lambda = 0.42$  in Avg.), reflecting a balanced trade-off between learning new features and preserving historical constraints.

Dataset	Mixing Coefficient $\lambda$																	
	0.1	0.2	0.3	0.4	<b>0.42</b>	0.44	0.46	0.48	0.5	0.52	0.54	0.56	0.58	0.6	0.7	0.8	0.9	
AIME25	7.8	10.0	12.2	16.7	<b>20.0</b>	20.0	16.7	20.0	20.0	21.1	16.7	16.7	16.7	10.0	20.0	20.0	12.2	
MATH500	71.4	67.1	70.8	73.1	<b>74.9</b>	74.5	73.2	73.3	73.3	70.7	74.0	73.0	73.3	68.9	71.7	70.9	66.1	
AQUA	77.2	72.8	74.7	75.2	<b>73.9</b>	73.1	72.4	71.8	73.9	71.0	71.3	71.9	70.2	64.8	66.9	61.4	60.8	
GSM8K	88.2	89.1	89.4	91.9	<b>91.8</b>	91.7	91.0	91.4	91.0	91.2	91.4	90.6	90.9	89.2	89.3	88.1	85.7	
MAWPS	94.9	96.6	95.5	97.8	<b>98.2</b>	97.8	97.8	98.0	95.7	96.5	97.2	96.8	97.5	94.7	96.2	95.5	93.6	
SVAMP	90.4	91.8	93.3	94.9	<b>94.1</b>	93.6	93.5	92.9	92.6	92.4	93.5	92.8	92.9	90.8	91.9	89.6	87.4	
Avg.	71.7	71.2	72.7	74.9	<b>75.5</b>	75.1	74.1	74.6	74.4	73.8	74.0	73.6	73.6	69.7	72.7	70.9	67.6	

**Table 6. Extended Logit Statistics Before vs. After Joint Training (Qwen3-4B-Base).** Weak = model 0, strong = model 1. “Pre” denotes before joint training, and “Stronger (Post)” denotes the jointly trained strong branch after training.  $\Delta$  denotes Post–Pre (percent change in parentheses). Centered norm values are taken directly from the logit analysis report.

Metric	Weak			Strong		
	Pre	Post	$\Delta$	Pre	Stronger (Post)	$\Delta$
Mean logit $z_{\text{mean}}$	3.65	9.42	5.77 (+158.1%)	2.87	0.97	-1.90 (-66.2%)
Std $\sigma$	3.06	2.65	-0.41 (-13.4%)	3.18	3.16	-0.02 (-0.6%)
Centered norm $\ \tilde{z}\ _2$	1191.33	1034.50	-156.83 (-13.2%)	1240.10	1229.79	-10.31 (-0.8%)
Max logit $z_{\text{max}}$	43.25	38.50	-4.75 (-11.0%)	48.75	60.50	11.75 (+24.1%)
Min logit $z_{\text{min}}$	-24.00	-22.50	1.50 (-6.2%)	-26.63	-35.75	-9.12 (+34.2%)
L2 norm $\ z\ _2$	1978.92	3858.60	1879.68 (+95.0%)	1865.96	1688.59	-177.37 (-9.5%)
Entropy $H$	0.52	2.43	1.91 (+367.3%)	0.44	0.48	0.04 (+9.1%)
Max prob $p_{\text{max}}$	0.83	0.53	-0.30 (-36.1%)	0.85	0.83	-0.02 (-2.4%)

### A.3. Extended Logit Statistics

To provide a more complete view of the logit dynamics underlying joint training, we report additional statistics from the logit analysis report in Table 6. Beyond the non-target logit mean reduction shown in Table 2, the extended metrics highlight a pronounced mean drift in the weak model and stable sharpness in the strong (post) model.

**Implementation details.** All logit statistics are computed from 200 randomly sampled examples drawn from the AM-1.4M training dataset used in our experiments. We run forward passes for the pre- and post-joint-training checkpoints on these examples and aggregate statistics across the sampled set. The centered-norm definition used in the table follows Appendix C (Eq. (56)).

## B. Supplementary Theory: Gradient Amplification under Logit Mixing

**Notation.** Fix a context  $x$  and a target token index  $y$ , and analyze a single joint-training step; we omit the conditioning on  $x$  for readability. The weak and strong models  $\mathcal{M}_{\text{weak}}$  and  $\mathcal{M}_{\text{strong}}$  produce logits  $z_{\text{weak}}(x), z_{\text{strong}}(x) \in \mathbb{R}^{|\mathcal{V}|}$ , and the mixed logits are  $z_{\text{mix}}(x) = (1 - \lambda)z_{\text{weak}}(x) + \lambda z_{\text{strong}}(x)$  with  $\lambda \in [0, 1]$ . For any logit map  $z(x)$ , define  $P_z(\cdot | x) = \text{Softmax}(z(x))$  and use the shorthand  $P_z(k)$ ; let  $e_y$  denote the one-hot target vector. We use a subscript  $i \in \{\text{weak, strong}\}$  to index the two models when writing model-agnostic expressions. For any negative token  $k \neq y$ , the margin is  $m_k(z(x)) = z(x)[y] - z(x)[k]$ .

### B.1. Setup and Baseline

We analyze joint training under logit mixing. The mixed logits are

$$z_{\text{mix}} = (1 - \lambda)z_{\text{weak}} + \lambda z_{\text{strong}}, \quad \lambda \in [0, 1]. \quad (23)$$

We distinguish the mixed-logit loss and the SFT loss on the strong model:

$$\mathcal{L}_{\text{mix}} = -\log P_{\text{mix}}(y), \quad \mathcal{L}_{\text{SFT}} = -\log P_{\text{strong}}(y), \quad (24)$$

where  $P_{\text{mix}} = P_{z_{\text{mix}}}$  and  $P_{\text{strong}} = P_{z_{\text{strong}}}$ . The joint-training gradient with respect to fused logits is

$$g_{\text{mix}} = \nabla_{z_{\text{mix}}} \mathcal{L}_{\text{mix}} = P_{\text{mix}}(\cdot) - e_y. \quad (25)$$

In standard SFT on the strong model alone, the corresponding gradient is

$$g_{\text{sft}} = \nabla_{z_{\text{strong}}} \mathcal{L}_{\text{SFT}} = P_{\text{strong}}(\cdot) - e_y. \quad (26)$$

For each model, gradients are scaled by the mixing coefficients:

$$\nabla_{z_{\text{weak}}} \mathcal{L}_{\text{mix}} = (1 - \lambda)g_{\text{mix}}, \quad \nabla_{z_{\text{strong}}} \mathcal{L}_{\text{mix}} = \lambda g_{\text{mix}}. \quad (27)$$

### B.2. Log-Odds and Margin Contraction

**Definition B.1** (Target margin). For any negative token  $k \neq y$ , define the margin

$$m_k(z) = z[y] - z[k]. \quad (28)$$

**Lemma B.2** (Softmax log-odds). For any  $k \neq y$ , the log-odds under logits  $z$  satisfy

$$\log \frac{P_z(k)}{P_z(y)} = -m_k(z). \quad (29)$$

*Proof.* By definition,  $P_z(k)/P_z(y) = \exp(z[k] - z[y]) = \exp(-m_k(z))$ .  $\square$

**Lemma B.3** (Margin mixing). For any  $k \neq y$ , the mixed margin equals the convex combination

$$m_k(z_{\text{mix}}) = (1 - \lambda)m_k(z_{\text{weak}}) + \lambda m_k(z_{\text{strong}}). \quad (30)$$

*Proof.* Using (23) and (28), we expand

$$\begin{aligned} m_k(z_{\text{mix}}) &= z_{\text{mix}}[y] - z_{\text{mix}}[k] \\ &= [(1 - \lambda)z_{\text{weak}}[y] + \lambda z_{\text{strong}}[y]] - [(1 - \lambda)z_{\text{weak}}[k] + \lambda z_{\text{strong}}[k]] \\ &= (1 - \lambda)(z_{\text{weak}}[y] - z_{\text{weak}}[k]) + \lambda(z_{\text{strong}}[y] - z_{\text{strong}}[k]) \\ &= (1 - \lambda)m_k(z_{\text{weak}}) + \lambda m_k(z_{\text{strong}}). \end{aligned} \quad (31)$$

$\square$

### B.3. Negative-Gradient Amplification

**Definition B.4** (Hard-negative set). Define the hard-negative set

$$\mathcal{H} = \{k \neq y : m_k(z_{\text{weak}}) < m_k(z_{\text{strong}})\}, \quad (32)$$

i.e., tokens for which the weak model has a smaller margin (more confusion).

**Lemma B.5** (Relative probability increase on hard negatives). *For any  $k \in \mathcal{H}$ ,*

$$\frac{P_{\text{mix}}(k)}{P_{\text{mix}}(y)} > \frac{P_{\text{strong}}(k)}{P_{\text{strong}}(y)}. \quad (33)$$

*Proof.* By (30),  $m_k(z_{\text{mix}}) < m_k(z_{\text{strong}})$  for  $k \in \mathcal{H}$ . Applying (29) yields a larger log-odds ratio for the mixed logits.  $\square$

**Corollary B.6** (Sufficient condition for per-token amplification). *For any  $k \in \mathcal{H}$ , the negative-token gradient on fused logits satisfies*

$$P_{\text{mix}}(k) \geq P_{\text{strong}}(k) \quad \text{whenever} \quad \frac{P_{\text{mix}}(y)}{P_{\text{strong}}(y)} \geq \exp(-(1-\lambda)\Delta m_k), \quad (34)$$

where  $\Delta m_k = m_k(z_{\text{strong}}) - m_k(z_{\text{weak}}) > 0$ .

*Proof.* We begin by expressing probabilities via log-odds (Lemma (29)):

$$\begin{aligned} \frac{P_{\text{mix}}(k)}{P_{\text{strong}}(k)} &= \frac{P_{\text{mix}}(y) \exp(-m_k(z_{\text{mix}}))}{P_{\text{strong}}(y) \exp(-m_k(z_{\text{strong}}))} \\ &= \frac{P_{\text{mix}}(y)}{P_{\text{strong}}(y)} \exp(m_k(z_{\text{strong}}) - m_k(z_{\text{mix}})). \end{aligned} \quad (35)$$

Using the margin mixing identity (Lemma (30)),

$$\begin{aligned} m_k(z_{\text{strong}}) - m_k(z_{\text{mix}}) &= m_k(z_{\text{strong}}) - [(1-\lambda)m_k(z_{\text{weak}}) + \lambda m_k(z_{\text{strong}})] \\ &= (1-\lambda)(m_k(z_{\text{strong}}) - m_k(z_{\text{weak}})) \\ &= (1-\lambda)\Delta m_k. \end{aligned} \quad (36)$$

Substituting (36) into (35) yields

$$\frac{P_{\text{mix}}(k)}{P_{\text{strong}}(k)} = \frac{P_{\text{mix}}(y)}{P_{\text{strong}}(y)} \exp((1-\lambda)\Delta m_k). \quad (37)$$

We now solve for the condition under which  $P_{\text{mix}}(k) \geq P_{\text{strong}}(k)$ :

$$\begin{aligned} \frac{P_{\text{mix}}(k)}{P_{\text{strong}}(k)} \geq 1 &\iff \frac{P_{\text{mix}}(y)}{P_{\text{strong}}(y)} \exp((1-\lambda)\Delta m_k) \geq 1 \\ &\iff \frac{P_{\text{mix}}(y)}{P_{\text{strong}}(y)} \geq \exp(-(1-\lambda)\Delta m_k). \end{aligned} \quad (38)$$

This is exactly the stated sufficient condition (34).  $\square$

**Theorem B.7** (Total negative-mass increase under uniform margin shrinkage). *If  $m_k(z_{\text{weak}}) \leq m_k(z_{\text{strong}})$  for all  $k \neq y$ , then*

$$P_{\text{mix}}(y) \leq P_{\text{strong}}(y) \quad \text{and} \quad \sum_{k \neq y} P_{\text{mix}}(k) \geq \sum_{k \neq y} P_{\text{strong}}(k). \quad (39)$$

*Proof.* By Lemma (30) and the assumption  $m_k(z_{\text{weak}}) \leq m_k(z_{\text{strong}})$ ,

$$m_k(z_{\text{mix}}) = (1-\lambda)m_k(z_{\text{weak}}) + \lambda m_k(z_{\text{strong}}) \leq m_k(z_{\text{strong}}) \quad \forall k \neq y. \quad (40)$$

Applying Lemma (29) yields, for each  $k \neq y$ ,

$$\exp(-m_k(z_{\text{mix}})) \geq \exp(-m_k(z_{\text{strong}})). \quad (41)$$

Summing (41) over  $k \neq y$  gives

$$\sum_{k \neq y} \exp(-m_k(z_{\text{mix}})) \geq \sum_{k \neq y} \exp(-m_k(z_{\text{strong}})). \quad (42)$$

Since

$$P_z(y) = \left(1 + \sum_{k \neq y} \exp(-m_k(z))\right)^{-1}, \quad (43)$$

the denominator for  $P_{\text{mix}}(y)$  is no smaller than that for  $P_{\text{strong}}(y)$ , and thus

$$P_{\text{mix}}(y) \leq P_{\text{strong}}(y). \quad (44)$$

Finally, because probabilities sum to one,

$$\sum_{k \neq y} P_{\text{mix}}(k) = 1 - P_{\text{mix}}(y) \geq 1 - P_{\text{strong}}(y) = \sum_{k \neq y} P_{\text{strong}}(k), \quad (45)$$

which proves (39).  $\square$

**Proposition B.8** (Logit updates emphasize negative suppression). *For any negative token  $k \neq y$ , the logit update for model  $i \in \{\text{weak, strong}\}$  under joint training is*

$$\Delta z_i[k] \approx -\eta s_i P_{\text{mix}}(k), \quad s_{\text{weak}} = 1 - \lambda, \quad s_{\text{strong}} = \lambda, \quad (46)$$

while for the target token,

$$\Delta z_i[y] \approx \eta s_i (1 - P_{\text{mix}}(y)). \quad (47)$$

Thus any increase in  $P_{\text{mix}}(k)$  directly amplifies the suppression of hard negatives, while a decrease in  $P_{\text{mix}}(y)$  strengthens the upward push on the target logit.

*Proof.* From (27), the model- $i$  logit gradient satisfies

$$\nabla_{z_i} \mathcal{L}_{\text{mix}} = s_i g_{\text{mix}}, \quad (48)$$

where  $g_{\text{mix}} = P_{\text{mix}}(\cdot) - e_y$  (Eq. (25)). For a negative token  $k \neq y$ , this gives

$$\frac{\partial \mathcal{L}_{\text{mix}}}{\partial z_i[k]} = s_i P_{\text{mix}}(k), \quad (49)$$

and for the target token,

$$\frac{\partial \mathcal{L}_{\text{mix}}}{\partial z_i[y]} = s_i (P_{\text{mix}}(y) - 1). \quad (50)$$

Under a first-order update  $\Delta z_i \approx -\eta \nabla_{z_i} \mathcal{L}_{\text{mix}}$ , we obtain

$$\Delta z_i[k] \approx -\eta s_i P_{\text{mix}}(k), \quad \Delta z_i[y] \approx \eta s_i (1 - P_{\text{mix}}(y)), \quad (51)$$

which matches (46) and (47).  $\square$

**Remark B.9** (Consistency with logits statistics). The logits evaluation report shows that after joint training the strong model exhibits lower mean logits and more extreme tails (e.g., larger magnitude minima and maxima). The mechanism above provides a local explanation: increased negative mass amplifies downward updates on many incorrect tokens, while the target receives a stronger upward push when  $P_{\text{mix}}(y)$  decreases. Mean shifts can further accumulate along shift-invariant directions (Appendix C).

Informally, this gradient amplification provides extra training signal compared to SFT, which helps reduce saturation and move optimization past local minima.

## C. Supplementary Theoretical Analysis of Joint Training Dynamics

### C.1. Problem Setting and Notation

**Notation.** Fix a context  $x$  and a target index  $y$ , and analyze a single joint-training step; we omit the conditioning on  $x$  for readability. The weak and strong models  $\mathcal{M}_{\text{weak}}$  and  $\mathcal{M}_{\text{strong}}$  have parameters  $\theta_{\text{weak}}$  and  $\theta_{\text{strong}}$ , and produce logits  $z_{\text{weak}}(x), z_{\text{strong}}(x) \in \mathbb{R}^{|\mathcal{V}|}$ . The mixed logits are

$$z_{\text{mix}} = (1 - \lambda)z_{\text{weak}} + \lambda z_{\text{strong}}, \quad \lambda \in [0, 1]. \quad (52)$$

For any logit map  $z(x)$ , define  $P_z(\cdot | x) = \text{Softmax}(z(x))$  and use the shorthand  $P_z(k)$ ; let  $P_{\text{mix}} = P_{z_{\text{mix}}}$  and  $e_y$  denote the one-hot target. We use a subscript  $i \in \{\text{weak, strong}\}$  to index the two models in generic expressions. Let  $\mathbf{1}$  be the all-ones vector in  $\mathbb{R}^{|\mathcal{V}|}$ . We use the mixed-logit loss

$$\mathcal{L}_{\text{mix}} = -\log P_{\text{mix}}(y), \quad (53)$$

and the residual

$$g = \nabla_{z_{\text{mix}}} \mathcal{L}_{\text{mix}} = P_{\text{mix}}(\cdot) - e_y. \quad (54)$$

For any negative token  $k \neq y$ , the margin is  $m_k(z) = z[y] - z[k]$ . We use  $\eta$  to denote the learning rate. For each model  $i \in \{\text{weak, strong}\}$ , let  $J_i = \partial z_i / \partial \theta_i$  and define the Jacobian Gram matrix

$$K_i = J_i J_i^\top. \quad (55)$$

**Definition C.1** (Centered logits and centered norm). Let  $\bar{z} = \frac{1}{|\mathcal{V}|} \mathbf{1}^\top z$  be the logit mean. The centered logits and centered norm are

$$\tilde{z} = z - \bar{z}\mathbf{1}, \quad \|\tilde{z}\|_2 = \sqrt{\sum_{k=1}^{|\mathcal{V}|} (z[k] - \bar{z})^2}. \quad (56)$$

Since  $\|\tilde{z}\|_2 = \sqrt{|\mathcal{V}|} \cdot \text{Std}(z)$ , the centered norm is a shift-invariant measure of sharpness.

### C.2. First-Order Gradients and Centered Linearized Dynamics

By the chain rule,

$$\nabla_{z_{\text{weak}}} \mathcal{L}_{\text{mix}} = (1 - \lambda)g, \quad (57)$$

$$\nabla_{z_{\text{strong}}} \mathcal{L}_{\text{mix}} = \lambda g. \quad (58)$$

Thus both models receive gradients in the same direction but with different magnitudes. Under a first-order (local) linearization, we apply a Taylor expansion of logits around  $\theta_i$ :

$$z_i(\theta_i + \Delta\theta_i) \approx z_i(\theta_i) + J_i \Delta\theta_i, \quad i \in \{\text{weak, strong}\}. \quad (59)$$

With  $\Delta\theta_i = -\eta \nabla_{\theta_i} \mathcal{L}_{\text{mix}}$ , this yields

$$\Delta z_i \approx -\eta J_i J_i^\top g = -\eta K_i g, \quad (60)$$

and incorporating the mixing weights in (57)–(58) yields

$$\Delta z_i \approx -\eta s_i K_i g, \quad s_{\text{weak}} = 1 - \lambda, \quad s_{\text{strong}} = \lambda. \quad (61)$$

To remove mean-shift effects, let  $\Pi = I - \frac{1}{|\mathcal{V}|} \mathbf{1} \mathbf{1}^\top$  be the centering projector. Since  $\mathbf{1}^\top g = 0$ , we have  $\Pi g = g$  and define the centered kernel

$$\tilde{K}_i = \Pi K_i \Pi. \quad (62)$$

Then the centered logit dynamics are

$$\Delta \tilde{z}_i \approx -\eta s_i \tilde{K}_i g. \quad (63)$$

**Lemma C.2** (PSD of centered kernel). *For each model  $i \in \{\text{weak, strong}\}$ ,  $\tilde{K}_i$  is positive semidefinite.*

*Proof.* For any  $x \in \mathbb{R}^{|\mathcal{V}|}$ ,  $x^\top \tilde{K}_i x = x^\top \Pi J_i J_i^\top \Pi x = \|J_i^\top \Pi x\|_2^2 \geq 0$ .  $\square$

The fused centered update is a doubly weighted combination of model updates:

$$\begin{aligned}\Delta \tilde{z}_{\text{mix}} &= (1 - \lambda) \Delta \tilde{z}_{\text{weak}} + \lambda \Delta \tilde{z}_{\text{strong}} \\ &= -\eta \left[ (1 - \lambda)^2 \tilde{K}_{\text{weak}} + \lambda^2 \tilde{K}_{\text{strong}} \right] g.\end{aligned}\quad (64)$$

The corresponding first-order loss decrease follows from a Taylor expansion of  $\mathcal{L}_{\text{mix}}$  at  $z_{\text{mix}}$ :

$$\Delta \mathcal{L}_{\text{mix}} \approx \nabla_{z_{\text{mix}}} \mathcal{L}_{\text{mix}}^\top \Delta \tilde{z}_{\text{mix}} = g^\top \Delta \tilde{z}_{\text{mix}}. \quad (65)$$

Substituting (64) gives

$$\Delta \mathcal{L}_{\text{mix}} \approx g^\top \Delta \tilde{z}_{\text{mix}} = -\eta \left[ (1 - \lambda)^2 g^\top \tilde{K}_{\text{weak}} g + \lambda^2 g^\top \tilde{K}_{\text{strong}} g \right]. \quad (66)$$

### C.3. Stage I: Hard-Negative Amplification and Strong-Model Dominance

Early in joint training, the weak model is more confused, so for many hard negatives  $k$  we have  $m_k(z_{\text{weak}}) < m_k(z_{\text{strong}})$ . By the logit-mixing analysis in Appendix B (e.g., Eq. (39)), mixing shrinks these margins and increases total negative probability mass. Consequently, the residual  $g$  grows in magnitude and is biased toward hard negatives: the weak model acts as a *gradient amplifier*, not a competitor in final accuracy.

The effective per-step loss decrease attributable to model  $i \in \{\text{weak, strong}\}$  is

$$E_i \triangleq \eta s_i^2 g^\top \tilde{K}_i g, \quad s_{\text{weak}} = 1 - \lambda, \quad s_{\text{strong}} = \lambda. \quad (67)$$

Dominance corresponds to  $E_{\text{strong}} > E_{\text{weak}}$ . Define the directional sensitivity  $\kappa_i = g^\top \tilde{K}_i g / \|g\|_2^2$ .

**Assumption C.3** (Sensitivity advantage of the strong model). Because the strong model is sharper (larger centered norm / lower entropy), its centered kernel responds more strongly along the residual direction:

$$g^\top \tilde{K}_{\text{strong}} g \approx \alpha g^\top \tilde{K}_{\text{weak}} g, \quad \alpha > 1. \quad (68)$$

Substituting (68) into (66) yields the total effective rate

$$S(\lambda) = (1 - \lambda)^2 + \alpha \lambda^2, \quad (69)$$

and the strong model dominates the joint update when

$$\lambda^2 \alpha > (1 - \lambda)^2. \quad (70)$$

Solving (70) gives the gradient-share crossover

$$\lambda_{\text{cross}} = \frac{1}{1 + \sqrt{\alpha}}. \quad (71)$$

*Remark C.4* (Crossover vs. accuracy). Equation (71) characterizes a *local* crossover of gradient contribution under a one-step linearization. It does *not* predict an accuracy inversion. In practice, both  $g$  and  $\tilde{K}_{\text{weak}}, \tilde{K}_{\text{strong}}$  evolve with  $\lambda$  and training time, while optimizer dynamics smooth the trajectory, yielding a broad optimum region rather than a sharp transition.

*Remark C.5* (Softmax amplification). Because  $P_{\text{mix}}(k) \propto \exp(z_{\text{mix}}[k])$ , modest logit differences can disproportionately tilt  $P_{\text{mix}}$  and  $g$ . This amplifies hard-negative gradients and reinforces the early dominance in (70).

### C.4. Stage II: Gradient Shielding via Hessian Contraction

We next analyze why the weak model loses effective training signal once the strong model becomes confident.

#### C.4.1. SOFTMAX JACOBIAN AND LOSS HESSIAN

Recall  $P_{\text{mix}} = \text{Softmax}(z_{\text{mix}})$ . The Jacobian of Softmax is

$$\frac{\partial P_{\text{mix}}}{\partial z_{\text{mix}}} = \text{diag}(P_{\text{mix}}) - P_{\text{mix}}P_{\text{mix}}^\top. \quad (72)$$

Since  $e_y$  is constant, the Hessian of the cross-entropy loss with respect to  $z_{\text{mix}}$  is

$$\mathbf{H}_{\mathcal{L}} = \nabla_{z_{\text{mix}}}^2 \mathcal{L}_{\text{mix}} = \frac{\partial(P_{\text{mix}} - e_y)}{\partial z_{\text{mix}}} = \text{diag}(P_{\text{mix}}) - P_{\text{mix}}P_{\text{mix}}^\top. \quad (73)$$

**Lemma C.6** (PSD of the loss Hessian).  $\mathbf{H}_{\mathcal{L}}$  is positive semidefinite.

*Proof.* For any  $v \in \mathbb{R}^{|\mathcal{V}|}$ ,

$$v^\top \mathbf{H}_{\mathcal{L}} v = \sum_j P_{\text{mix}}[j] v_j^2 - \left( \sum_j P_{\text{mix}}[j] v_j \right)^2 = \text{Var}_{P_{\text{mix}}}(v) \geq 0. \quad (74)$$

□

#### C.4.2. INTERACTION HESSIAN BETWEEN MODELS

The mixed logits depend on both models, so the cross-Hessian captures how updates in the strong model affect the gradient seen by the weak model:

$$\begin{aligned} \mathbf{H}_{\text{ws}} &= \frac{\partial}{\partial z_{\text{strong}}} [\nabla_{z_{\text{weak}}} \mathcal{L}_{\text{mix}}] \\ &= (1 - \lambda) \frac{\partial(P_{\text{mix}} - e_y)}{\partial z_{\text{mix}}} \frac{\partial z_{\text{mix}}}{\partial z_{\text{strong}}} \\ &= \lambda(1 - \lambda) \mathbf{H}_{\mathcal{L}}. \end{aligned} \quad (75)$$

#### C.4.3. SHIELDING IN THE CONFIDENT REGIME

Assume the target index is  $y$  and the strong model drives the mixed prediction to  $P_{\text{mix}}(y) \rightarrow 1$ . Then  $P_{\text{mix}}(k) \rightarrow 0$  for all  $k \neq y$ , which implies

$$\lim_{P_{\text{mix}} \rightarrow e_y} \mathbf{H}_{\mathcal{L}} = \mathbf{0}. \quad (76)$$

Consequently,

$$\lim_{P_{\text{mix}} \rightarrow e_y} \mathbf{H}_{\text{ws}} = \mathbf{0}, \quad (77)$$

and the weak model receives vanishing curvature information. This is the mathematical form of *gradient shielding*: once the strong model dominates and the prediction saturates, both the first-order residual  $g$  and its local sensitivity collapse, making it difficult for the weak model to receive informative updates.

### C.5. Stage III: Null-Space Drift and Mean Shift

We now explain the observed mean drift of the weak model logits.

#### C.5.1. SHIFT INVARIANCE OF THE MIXED SOFTMAX

Softmax is invariant to global shifts. For any scalar  $c$ ,

$$\text{Softmax}(z + c\mathbf{1}) = \text{Softmax}(z). \quad (78)$$

Applying this to the fused logits, let  $z'_{\text{weak}} = z_{\text{weak}} + c\mathbf{1}$ . Then

$$\begin{aligned} z'_{\text{mix}} &= (1 - \lambda)z'_{\text{weak}} + \lambda z_{\text{strong}} \\ &= z_{\text{mix}} + (1 - \lambda)c\mathbf{1}, \end{aligned} \quad (79)$$

and by (78) the predictive distribution is unchanged. Hence, the loss is flat along the mean-shift direction of each model.

### C.5.2. ZERO-EIGENVALUE DIRECTION OF THE HESSIAN

Let  $\mathbf{1}$  denote the all-ones vector. From (73),

$$\mathbf{H}_{\mathcal{L}} \mathbf{1} = \text{diag}(P_{\text{mix}}) \mathbf{1} - P_{\text{mix}}(P_{\text{mix}}^\top \mathbf{1}) = P_{\text{mix}} - P_{\text{mix}} = \mathbf{0}. \quad (80)$$

Thus  $\mathbf{1}$  is a zero-eigenvalue direction of the Hessian, confirming that the loss has no curvature along global shifts.

### C.5.3. WHY DRIFT ACCUMULATES IN THE NULL SPACE

When the strong model has already fit the data, the expected gradient seen by the weak model is near zero. With stochastic training, the update can be modeled as

$$\theta^+ = \theta - \eta \epsilon, \quad \epsilon \sim \mathcal{N}(0, \Sigma), \quad (81)$$

which is a random walk. The logit space decomposes as

$$z = \bar{z} \mathbf{1} + \tilde{z}, \quad \tilde{z}^\top \mathbf{1} = 0, \quad (82)$$

where the null space is  $\text{span}\{\mathbf{1}\}$  and the active space is its orthogonal complement. In the active space, even small gradients can weakly restore the distribution shape. In the null space, there is no restoring force; thus the variance of  $\tilde{z}$  grows with time, leading to the observed mean drift without a corresponding increase in centered norm.

## D. System Prompts

We employ a specific system prompt to enforce the Chain-of-Thought (CoT) reasoning format. The exact instruction provided to the model is detailed in Table 7.

---

### System Prompt for Reasoning Enforcement

---

You are a helpful assistant. To answer the user's question, you first think about the reasoning process and then provide the user with the answer. The reasoning process and answer are enclosed within `<think>` and `<answer>` tags, respectively, i.e., `<think>` reasoning process here `</think>` `<answer>` answer here `</answer>`.

Table 7. The system prompt used to guide the model's output structure, ensuring distinct separation between internal reasoning and the final response.

## E. Data Construction

High-quality data is pivotal for effective alignment. We construct our training mixture from two primary domains: mathematics and code.

- **Mathematical Reasoning:** We source our math corpus from the AM-1.4M dataset (Zhao et al., 2025). To ensure the rigor of the reasoning chains, we utilized the `math_verify` library to rigorously parse and cross-check final solutions against ground truths. Only samples that successfully passed this verification were retained, resulting in **111,709** high-quality samples.
- **Code Generation:** For the coding domain, we curated data from AM-1.4M dataset. We implemented an **execution-based filtering pipeline**: code blocks were explicitly extracted from the responses and validated against corresponding test cases to ensure functional correctness. After deduplication and strict quality control, we obtained **104,077** valid code samples.

In total, the curated dataset comprises approximately 215k samples. We conducted training and evaluation for both tasks independently. Unless otherwise specified, all results reported in the main text are obtained by training with a sequence length of 8192 tokens and evaluating with 4096 tokens. In addition, we consider two aligned context-length settings—4k/4k and 8k/8k—under which our method also demonstrates consistent effectiveness.